

© 1986 Society of Photo-Optical Instrumentation Engineers.

This paper was published in SPIE Proceedings Volume 684 and is made available as an electronic reprint with permission of SPIE. One print or electronic copy may be made for personal use only. Systematic or multiple reproduction, distribution to multiple locations via electronic or other means, duplication of any material in this paper for a fee or for commercial purposes, or modification of the content of the paper are prohibited.

## Ferroelectric liquid-crystal and fast nematic spatial light modulators

D. Armitage and J. I. Thackara

Lockheed Missiles & Space Company, Inc., Research & Development Division,  
Palo Alto, CA 94304

N. A. Clark and M. A. Handschy

Displaytech, Inc., 2200 Central Avenue, Boulder, CO 80301

### Abstract

The electro-optic display industry has developed liquid-crystal technology to the level of TV imaging. For optical processing and other special applications, a much faster response time is desirable. Techniques which optimize the response of nematic liquid crystals are reviewed. Ferroelectric liquid crystals are described, with which switching speeds well beyond nematic limitation are achieved. A photoaddressed spatial light modulator using bismuth silicon oxide as the photoconductor addressing a surface-stabilized ferroelectric liquid crystal is described. Initial experimental results are presented.

### Introduction

Several liquid-crystal phases are illustrated in Figure 1.<sup>1</sup> At sufficiently high temperature, long-range order is absent and the fluid properties are isotropic. At lower temperature, the rod-like molecules of the nematic phase have long-range orientational order, which is associated with substantial birefringence or dielectric anisotropy. Chirality at the molecular level gives rise to a twisted nematic structure or cholesteric phase.

The smectic phases are associated with the onset of positional correlations and a layered structure. The smectic-C phase ( $S_C$ ) is distinguished from the smectic-A phase ( $S_A$ ) by tilt relative to the layers. Introduction of chirality in  $S_C$  produces the spiral version ( $S_C^*$ ) shown in Figure 2. The  $S_C^*$  symmetry accommodates ferroelectricity, allowing a bulk dipole moment orthogonal to the tilt direction and parallel to the layer. The polarization  $P$  spirals in accordance with the chirality of the phase.<sup>2</sup>

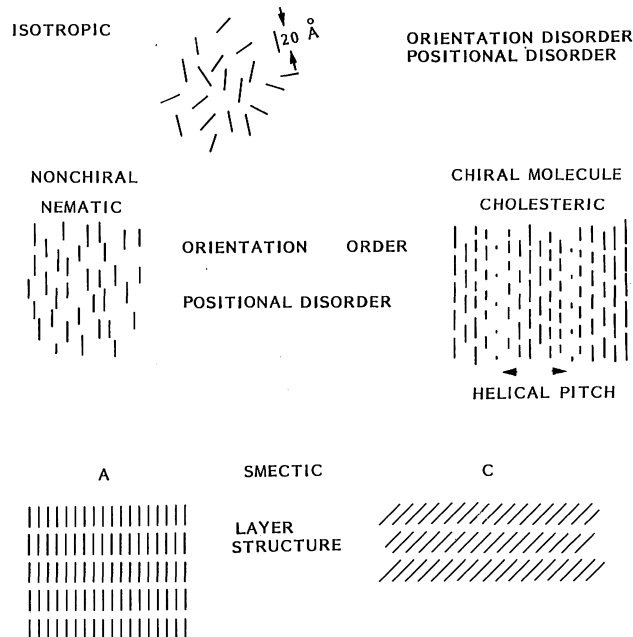


Figure 1. Liquid-crystal phases.

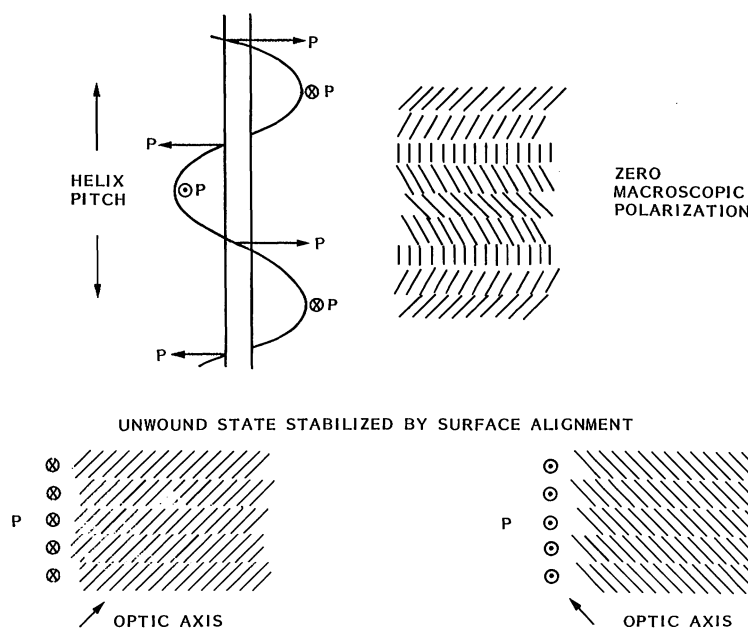


Figure 2. Chiral smectic-c ferroelectric liquid-crystal phase.

In the display and electro-optics industry, liquid crystals are identified with birefringent modulation at low voltage and low energy. The nematic liquid crystal (NLC) technology is maturing so that video rates are readily achieved in a variety of TV displays now available. For optical processing or other special applications, much faster rates are desirable.

Room-temperature ferroelectric liquid crystals (FLC) are now readily available, prompting an expansion in device activity.<sup>3</sup> The current FLC device response time is approaching 1  $\mu$ s, and, with continuing materials development, substantially higher speeds are expected.

#### Fast nematic devices

The NLC responds to an applied electric field via an induced dipole mechanism, which results in a square law torque dependence.<sup>1</sup>

$$\text{torque} = \Delta\epsilon E^2 \sin\phi \cos\phi \quad (1)$$

where:

$\Delta\epsilon = \epsilon_{\parallel} - \epsilon_{\perp}$  = permittivity anisotropy  
 $E$  = applied electric field  
 $\phi$  = nematic orientation  $\hat{n}$  relative to  $E$

The NLC response is limited by viscoelastic forces.

$$\text{torque} = K d^2\hat{n}/dz^2 + \eta d\hat{n}/dt \quad (2)$$

where:

$K$  = elastic constant  
 $\hat{n}$  = nematic director which identifies the local orientation  
 $z$  = spatial coordinate  
 $\eta$  = viscosity

This is a considerable simplification of NLC viscoelasticity, but suffices for most device work.<sup>1</sup>

The typical NLC device provides a drive-on state, determined by the applied voltage. When the voltage is removed, the drive-on state relaxes to an off state at a rate limited

by viscoelasticity. The drive-on time can be reduced by increasing the voltage, but the relaxation time is determined by material properties and geometry. If  $\Delta\epsilon$  changes signs with frequency, Eq. (1) shows that drive-on and drive-off can be achieved by frequency switching the applied voltage.<sup>1</sup> Materials with appropriate  $\Delta\epsilon$  are available, but this approach is unpopular due to the additional drive complexity, and power required.

Fast response favors a thin cell, as indicated in the expressions for a parallel aligned cell similar to that shown in Figure 3.<sup>1</sup>

$$\tau_r = \eta L^2 / (\Delta\epsilon V^2 - K\pi^2) \quad (3)$$

$$\tau_d = \eta L^2 / K\pi^2 \quad (4)$$

where:

- $\tau_r$  = rise time
- $\tau_d$  = decay time
- $L$  = cell thickness
- $V$  = applied voltage

Equation (3) is an underestimate when the initial conditions put  $E$  orthogonal to  $\hat{n}$ , giving zero torque in Eq. (1). Reducing  $L$  trades dynamic range for speed, but other factors determining cell thickness usually predominate.

Fast birefringent modulation can be achieved by switching the drive voltage between voltage levels  $V$  and  $V_0$ . The decay time constant can then be written<sup>4</sup>

$$\tau_d = (\eta L^2 / K) / [(V_0 / V_c)^2 + 1] \quad (5)$$

where

- $V_0$  = off-state voltage  $< V$  = on-state voltage
- $V_c$  = critical voltage =  $\pi(K/\Delta\epsilon)^{1/2} \approx 1$  V

With  $V_0$  applied, the NLC is almost entirely aligned along the field direction except at the cell boundary region where strong parallel surface alignment prevails, as shown in Figure 3. Readout light propagating perpendicular to the cell wall sees only the birefringence of the surface region. Switching to the higher voltage modulates the birefringence by further depletion of the surface birefringent region.<sup>5</sup> This surface-mode device also favors fast drive-on since the active region approximates  $\phi = 45^\circ$  in Eq. (1). The  $\pi$ -cell variant, with opposed tilt alignment, is advantageous for off-axis viewing in display applications.<sup>6</sup> The voltage levels are determined by the required dynamic range, where speed can be traded for range. Drive-on times of order 100  $\mu$ s at 1-kHz frame rates have been demonstrated.<sup>7</sup>

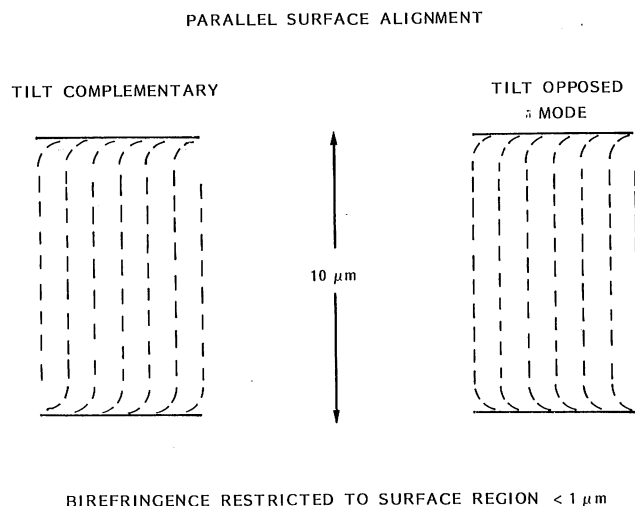


Figure 3. Surface-mode liquid-crystal cells.

Drive-on and drive-off can be achieved by switching the field direction as shown in Figure 4. Application of this technique generally requires an interdigitated electrode structure.<sup>8</sup> A transverse component of field is readily achieved in the photoaddressed spatial light modulator, which can consequently function as a spatially differentiating or edge enhancing device.<sup>9</sup> This technique can push the frame rate beyond 1 kHz.

In general the synthesis of NLC compounds is well established and further developments are not expected to improve the response speed significantly.

### Ferroelectric liquid-crystal device

The helical ferroelectric phase shown in Figure 2 has zero net polarization on a scale greater than the pitch length, which is typically of micrometer order. The helix can be unwound by an applied electric field and would constitute an electro-optic effect; however the process is associated with disclination structures which slow the response.

The surface-stabilized ferroelectric liquid-crystal (SSFLC) device structure is shown in Figures 2 and 5.<sup>10</sup> Here the helix is unwound by surface alignment forces when the cell thickness is comparable with the pitch length. The optic axis switches through twice the  $S_C^*$  tilt angle when the polarization is reversed, as shown in Figure 5. This is achieved by molecular rotation in the smectic layers with a minimum of viscoelastic retardation. Amplitude modulation is achieved by the crossed polarizer configuration indicated in Figure 5. For maximum contrast the FLC is molecularly engineered to have a 22.5° tilt angle.

If the surface alignment influence is modest, the alternate orientations can be stored and bistable switching is initiated by a positive or negative voltage pulse. The first-order coupling of the FLC polarization and applied electric field gives a torque expression:

$$\text{torque} = P E \sin\psi \tag{6}$$

where:

- P = FLC polarization
- E = applied electric field
- $\psi$  = angular relation of P and E

The torque now follows the sign of E (in contrast to Eq. (1) for NLC), allowing rapid switching in either direction. The switching speed is viscous limited according to the expression

$$\tau \approx \eta/PE \tag{7}$$

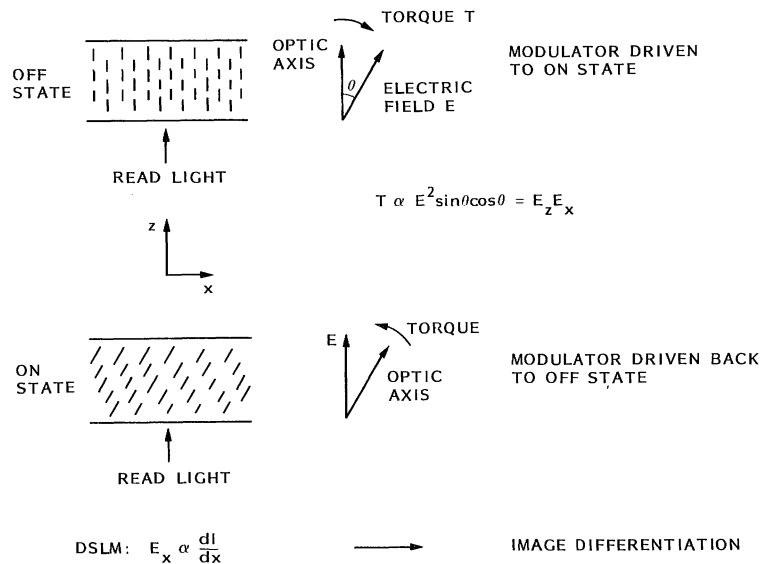


Figure 4. Perpendicularly aligned liquid-crystal structure with on/off drive capability and image differentiating effect.

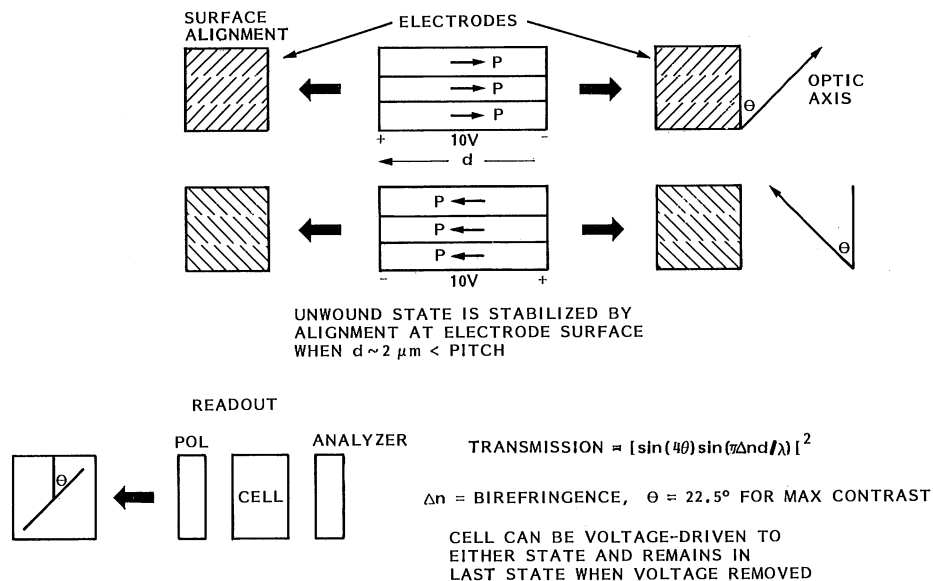


Figure 5. Surface-stabilized ferroelectric liquid-crystal device.

The advantage in switching speed of FLC over NLC lies in the large polarization which interacts directly with the applied field.

The bistability and well defined threshold of the SSFLC device are ideal for large-scale passive matrix-addressing. Considerable effort is being expended worldwide to develop a large-scale matrix-addressed SSFLC device for display purposes. Several prototypes have been demonstrated.<sup>2</sup>

The photoaddressed SSFLC spatial light modulator (SLM) has been neglected in comparison with matrix-addressing. Such devices are of value in optical processing applications. Our initial results appear to be the first publication in this field.<sup>11</sup>

The alignment of a NLC in contact or close to a surface is determined by physiochemical interactions. The alignment can be controlled by surface coatings and surface anisotropy introduced by unidirectional rubbing or oblique evaporation methods.<sup>1</sup> Several techniques are established and have been incorporated in the fabrication technology of the NLC display industry.

Although these techniques have some influence, they seem inadequate for the SSFLC device. In general the smectic phase is less forgiving of alignment perturbations than the nematic; moreover, bistability requires a delicate alignment that can store alternate orientations. The rubbed polymer process is the most popular procedure currently employed.<sup>12</sup>

Switching speeds of 10  $\mu\text{s}$  have been achieved with available stable compounds at room temperature. New compounds under development are pushing the speed to 1  $\mu\text{s}$ .

### Experimental

Bismuth silicon oxide (BSO) has been employed as the photoaddressing element in a NLC-SLM.<sup>13</sup> BSO has the advantage of ease of fabrication, high resolution, and extreme dark resistivity. The optically polished surface of BSO is of some advantage as an alignment basis for the SSFLC. The long detrapping times in BSO limit the frame rates to order 10 Hz.

Figure 6 illustrates the device structure. The BSO crystal (Sumitomo) is capacitively coupled by a thin optical cement bond to the transparent indium tin oxide (ITO) electrode coating the massive glass substrate. The crystal dimensions are 25 mm square by 1/2 mm thick, and both surfaces are optically polished. The counter electrode is formed from a similar ITO coating on glass. The FLC employed is a 50/50 mixture of compounds W7 and W82 (Displaytech).<sup>14</sup> This FLC aligns perpendicularly on BSO, necessitating the use of a coating to induce parallel alignment. A solution of 6/9 nylon in cresol/methanol is spun onto the exposed BSO and ITO surfaces, followed by drying and unidirectional rubbing.<sup>12</sup>

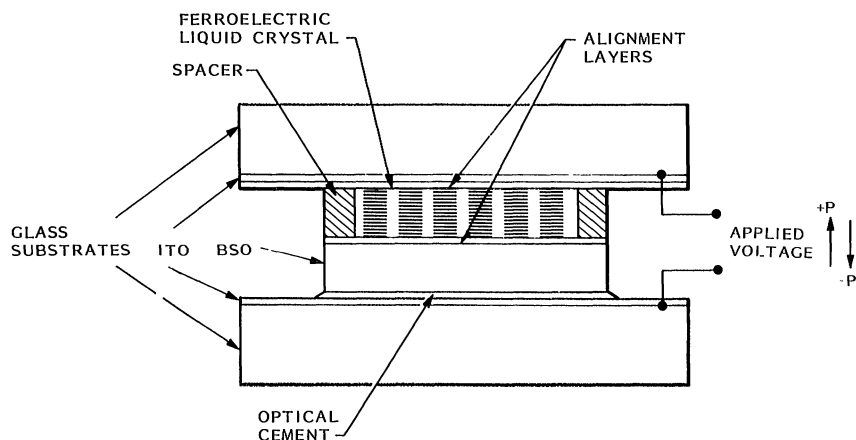


Figure 6. Bismuth silicon oxide photoaddressed ferroelectric liquid-crystal spatial light modulator.

SSFLC requires a cell spacing of micrometer order for the FLC employed. Because the viscosity of the FLC is sufficient to maintain the gap in the absence of a spacer, the initial experiments were performed without a spacer. The device is assembled by placing a drop of FLC between the BSO and the counter-electrode surfaces. The temperature is then raised to 60°C, which is beyond the isotropic point of the FLC. After cooling to room temperature, the FLC alignment was observed with polarized-light microscopy.

The SLM test bed is shown in Figures 7 and 8. The acousto-optic modulators switch write and read pulses of controllable length. The write pulse is applied via a Twyman-Green interferometer which controls the SLM input spatial frequency. Alternatively, a transparency or resolution chart can be imaged onto the input plane. The optical pulses are synchronized to the SLM activating voltage via controllable delays.

TV cameras view the output image and Fourier planes. Alternatively, the output can be imaged directly onto photographic film.

The image is written in the BSO with a green argon-laser light pulse and read continuously with red helium-neon light. The BSO is insensitive to red light. In this case the green light is isolated from the read plane by a dichroic filter.

### Results

The first SLM devices are switched at video rates and beyond with 10 V dc applied, under white-light illumination, in a crossed polarizer environment. Bistability or storage is virtually absent.

A transient image, which fades over a period of seconds, is observed in the SLM test bed. This fading is interpreted as space-charge accumulation effects in the BSO. The behavior remains essentially the same for a variety of applied voltage waveforms, including ac, up to a maximum of 100 V.

For weaker aligned samples, video rate switching is seen as before in white-light illumination, but significant storage is present. In the SLM test bed, a permanent image is now written which can be stored for several hours or more. However, there is still failure to switch cyclically under ac applied-voltage conditions.

The refreshed image in Figure 9 shows the USAF 1951 resolution test target immediately after writing. Lack of uniformity in this image is associated with variations in FLC thickness and alignment. Figure 9 also compares the refreshed image with the same image stored overnight for 15 h. The storage is assessed with the BSO completely discharged by optical exposure. Deterioration in the stored image is probably associated with surface alignment problems.

Figure 10 shows polarizing-microscope pictures of the stored resolution test image. The large number of defects illustrates the inadequacy of the alignment technique in these initial experiments.

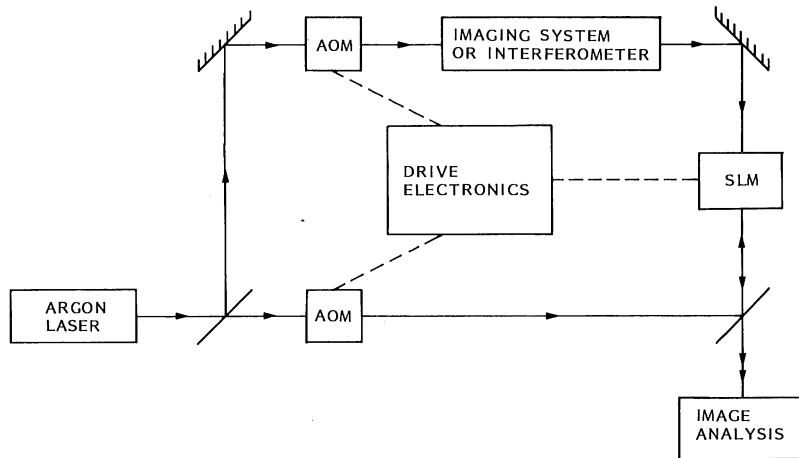


Figure 7. Simplified spatial light modulator test bed.

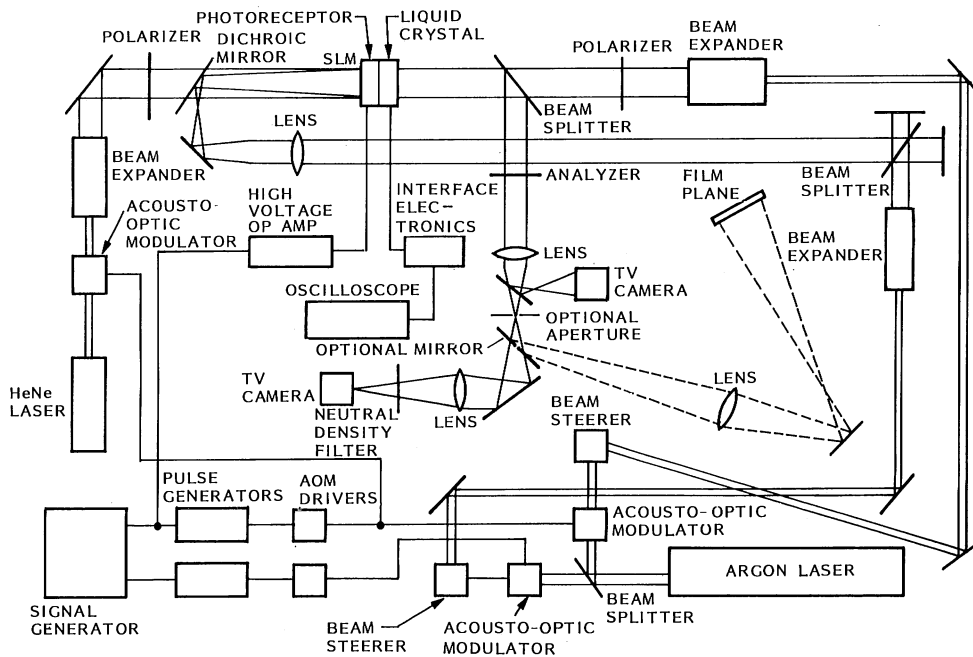


Figure 8. Complete spatial light modulator test bed.

Similar experiments employing amorphous selenium as the photoaddressing medium show transient imaging. This is similar to the initial BSO experiments and can again be interpreted as space-charge effects in the selenium.

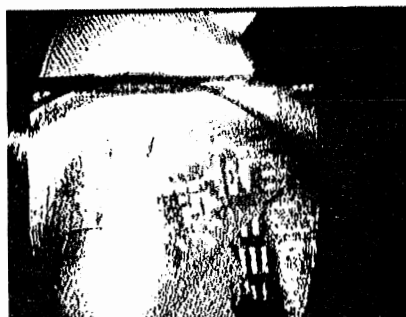
We have initiated experiments in a silicon photoaddressing technology which should allow the full speed potential of the FLC to be realized.<sup>15</sup> With crystalline silicon, space-charge effects are absent and cyclic switching is observed. We have recorded beyond 10 lp/mm resolution in a silicon photoaddressed SSFLC-SLM.

#### Acknowledgment

The advice and comments of W. W. Anderson and J. H. Becker are appreciated and discussion with M. E. Stefanov on liquid-crystal aspects is acknowledged. The work is supported by a Lockheed internal research program.



REFRESH



OVERNIGHT  
STORAGE

Figure 9. SSFLC-SLM refreshed image and stored image.

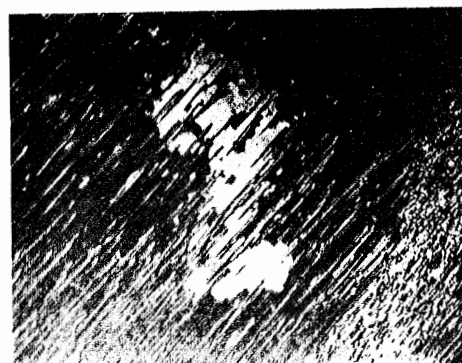
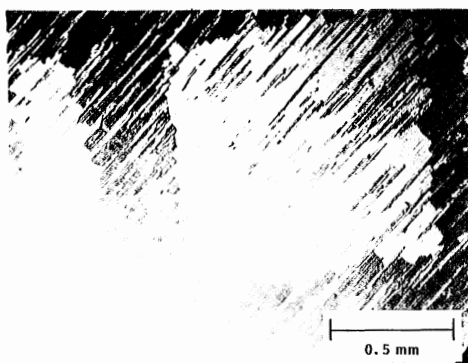


Figure 10. Polarizing microscope pictures of SSFLC-SLM stored image.

#### References

1. Priestley, E. B., Wojtowicz, P. J., Sheng, P., (Editors), Introduction to Liquid Crystals, Plenum, New York, 1974.
2. Clark, N. A., Lagerwall, S. T., "Physics of Ferroelectric Fluids: The Discovery of High-Speed Electrooptic Switching Process in Liquid Crystals," Recent Developments in Condensed Matter Physics, Vol. 4, pp. 309-319, 1981.
3. Clark, N. A., Lagerwall, S. T., Wahl, J., "Modulators Linear Arrays, and Matrix Arrays Using Ferroelectric Liquid Crystals," SID Digest, Vol. 26, pp. 133-136, 1985.
4. Pieranski, P., Brochard, F., Guyon, E., "Static and Dynamic Behavior of a Nematic Liquid Crystal in a Magnetic Field, Part 2: Dynamics," J. Phys. (Paris), Vol. 34, pp. 35-48, 1973.
5. Ferguson, J. L., "Performance of Matrix Display Using Surface Mode," Conference Record Biennial Display Research, pp. 177-182, 1980.
6. Bos, P. J., Johnson, P. A., Koehler/Beran, K. R., "The -Cell: A New, Fast Liquid-Crystal Optical-Switching Device," Mol. Cryst. Liq. Cryst., V 113, pp. 329-337, 1985.
7. Armitage, D., Stefanov, M. E., "Fast Liquid Crystal Modulator," CLEO Tech. Digest, pp. 44-45, 1985.
8. Channin, D. J., Carlson, D. E., "Rapid Turn-Off in Triode Optical Gate Liquid Crystal Devices," App. Phys. Lett., Vol. 28, pp. 300-302, 1976.
9. Armitage, D., Thackara, J. I., "Liquid-Crystal Differentiating Spatial Light Modulator," SPIE Nonlinear Optics & Applications, Vol. 613, pp. 165-171, 1986.
10. Clark, N. A., Lagerwall, S. T., "Submicrosecond Bistable Electrooptic Switching in Liquid Crystals," App. Phys. Lett., Vol. 36, pp. 899-901, 1980.
11. Armitage, D., Thackara, J. I., Clark, N. A., Handschy, M. D., "Ferroelectric Liquid Crystal-Photoaddressed Spatial Light Modulator," CLEO Tech. Digest, pp. 366, 1986.
12. Patel, J. S., Leslie, T. M., Goodby, J. W., "A Reliable Method of Alignment for Smectic Liquid Crystals," Ferroelectrics, Vol. 59, pp. 137-144, 1984.

13. Auberg, P., Huignard, J. P., Hareng, M., Mullen, R. A., "Liquid Crystal Light Valve Using Bulk Monocrystalline  $\text{Bi}_{12}\text{SiO}_{20}$  as the Photoconductive Material," App. Opt., Vol. 21, pp. 3706-3712, 1982.
14. Walba, J. M., Slater, S. C., Thurmes, W., Clark, N. A., Hanschy, M. A., Supon, F., "Design and Synthesis of a New Ferroelectric Liquid Crystal Family: Liquid Crystals Containing a Nonrecomic 2-Alkoxy-1-Propoxy Unit," J. Am. Chem. Soc., In Press, 1986.
15. Armitage, D., Anderson, W. W., Karr, T. J., "High Speed Spatial Light Modulator," IEEE J. Q. E., QE-21, pp. 1241-1248, 1985.





